
Figures and figure supplements

Activation-triggered subunit exchange between CaMKII holoenzymes facilitates the spread of kinase activity

Margaret Stratton, et al.

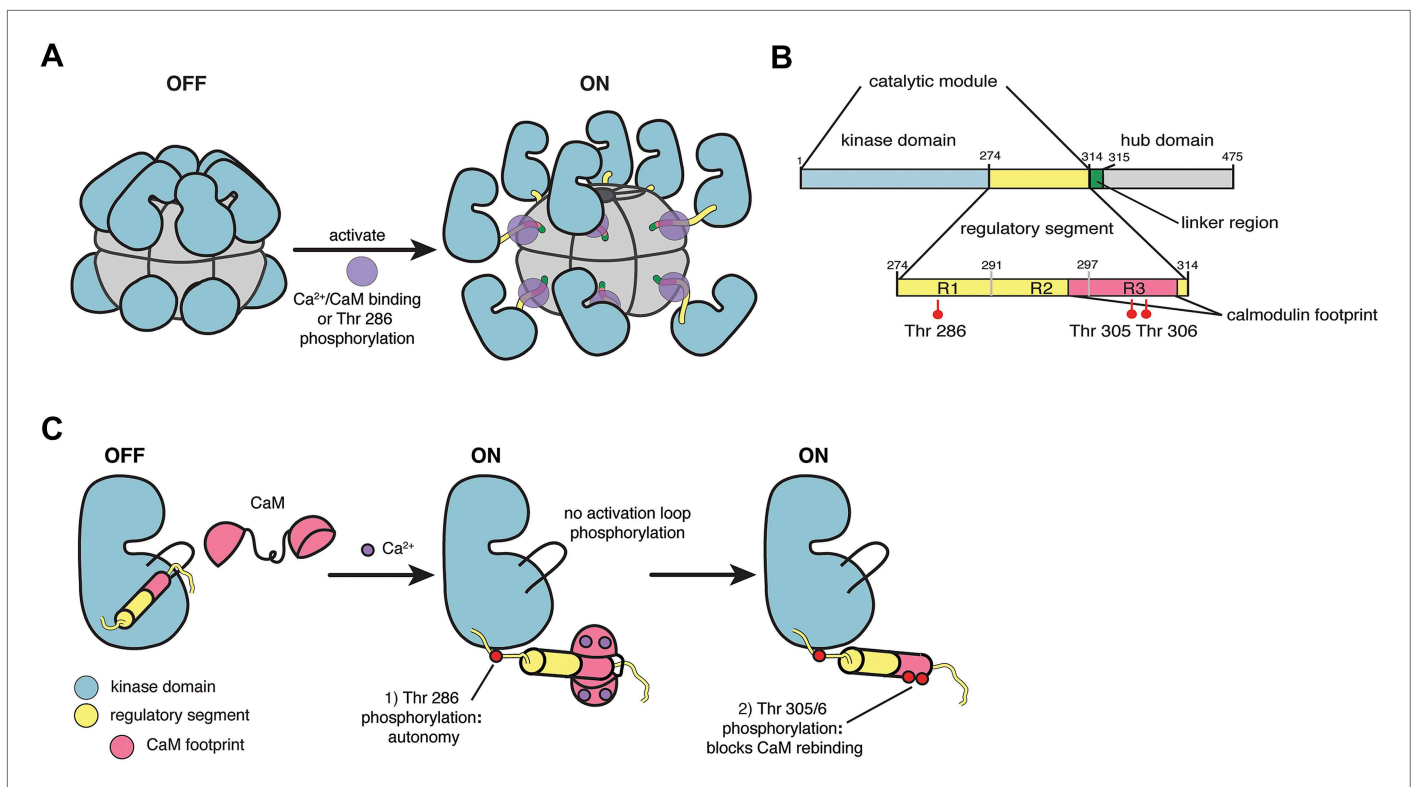


Figure 1. CaMKII architecture. **(A)** The architecture of a dodecameric CaMKII holoenzyme. The inactive holoenzyme is shown as a more compact configuration. Upon activation by Ca²⁺/CaM, or phosphorylation of Thr 286 in the regulatory segment (purple circles), the kinase domains are extended from the hub assembly. **(B)** The domains of a CaMKII subunit. **(C)** Phosphorylation control in CaMKII. The R1 element of the regulatory segment leads into a helical R2 element that blocks the substrate binding channel of the kinase domain in the inactive form. The R3 element contains the calmodulin-recognition motif, and upon CaM binding, CaMKII is autophosphorylated at Thr 286 in the R1 element. After CaM dissociates, Thr 305 and 306 are phosphorylated if Thr 286 is already phosphorylated.

DOI: [10.7554/eLife.01610.003](https://doi.org/10.7554/eLife.01610.003)

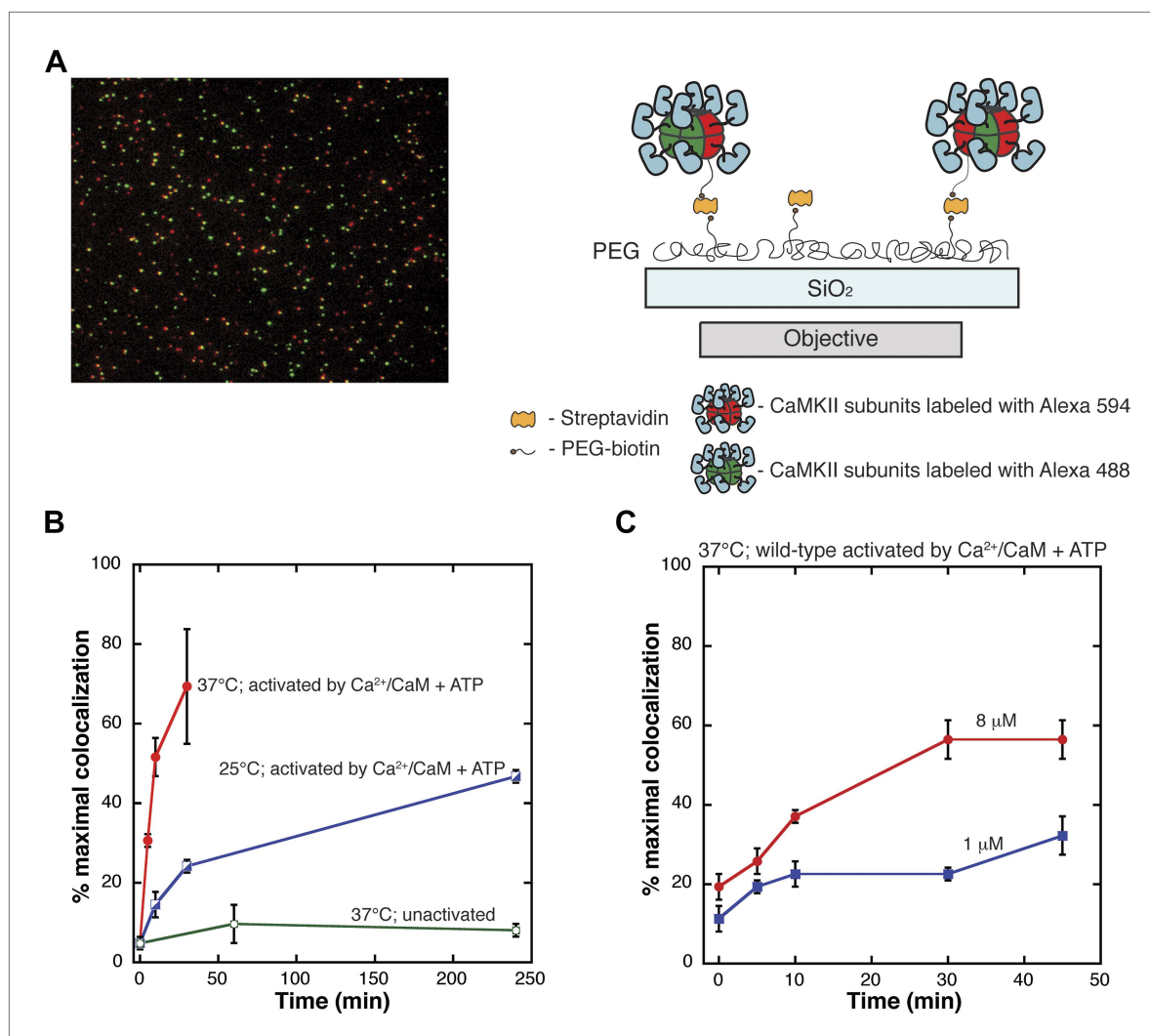


Figure 2. Single-molecule assay for subunit exchange reveals activation-dependent subunit exchange. **(A)** A representative single-molecule TIRF image, with red and green channels overlaid (left). For analysis, CaMKII holoenzymes are immobilized on glass slides via biotin/streptavidin interactions (right). **(B)** The rate of increase in colocalization is significantly faster at 37°C (red) compared to 25°C (blue) when Ca²⁺/CaM and ATP are added. At 37°C, the unactivated sample (i.e., with no addition of Ca²⁺/CaM and ATP) shows only a low level of exchange even at long time points (green). **(C)** Under activating conditions, decreasing the concentration of CaMKII from 8 μM (red) to 1 μM (blue) results in reduction of the rate of colocalization.

DOI: [10.7554/eLife.01610.004](https://doi.org/10.7554/eLife.01610.004)

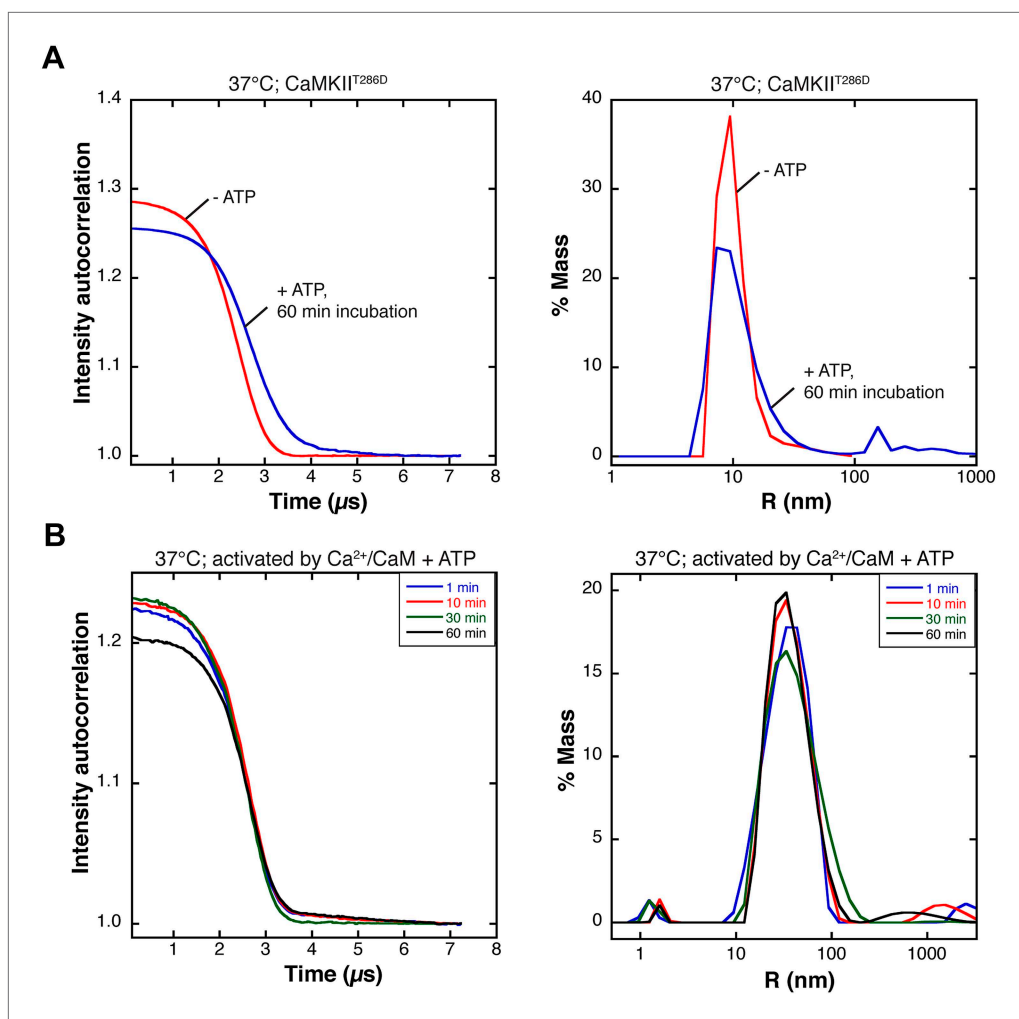


Figure 2—figure supplement 1. Dynamic light scattering measurements on CaMKII.

DOI: [10.7554/eLife.01610.005](https://doi.org/10.7554/eLife.01610.005)

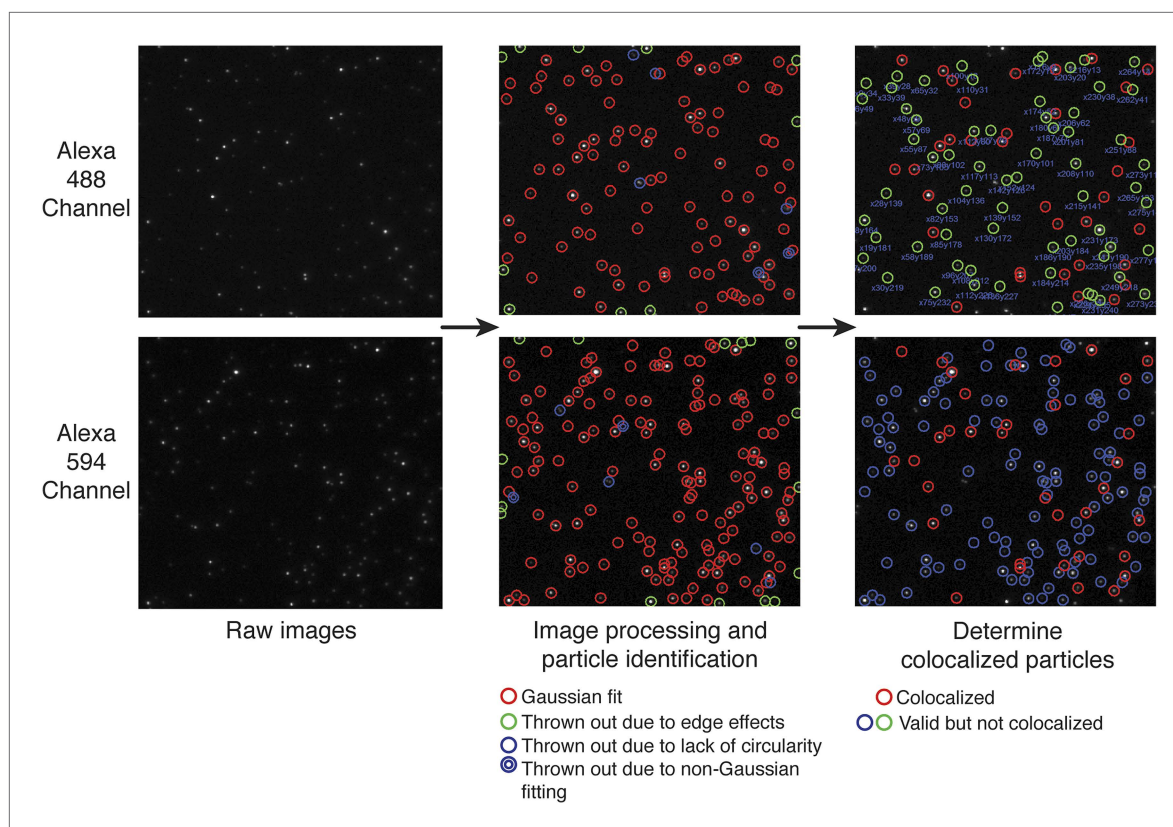


Figure 2—figure supplement 2. Custom particle-tracking program.

DOI: [10.7554/eLife.01610.006](https://doi.org/10.7554/eLife.01610.006)

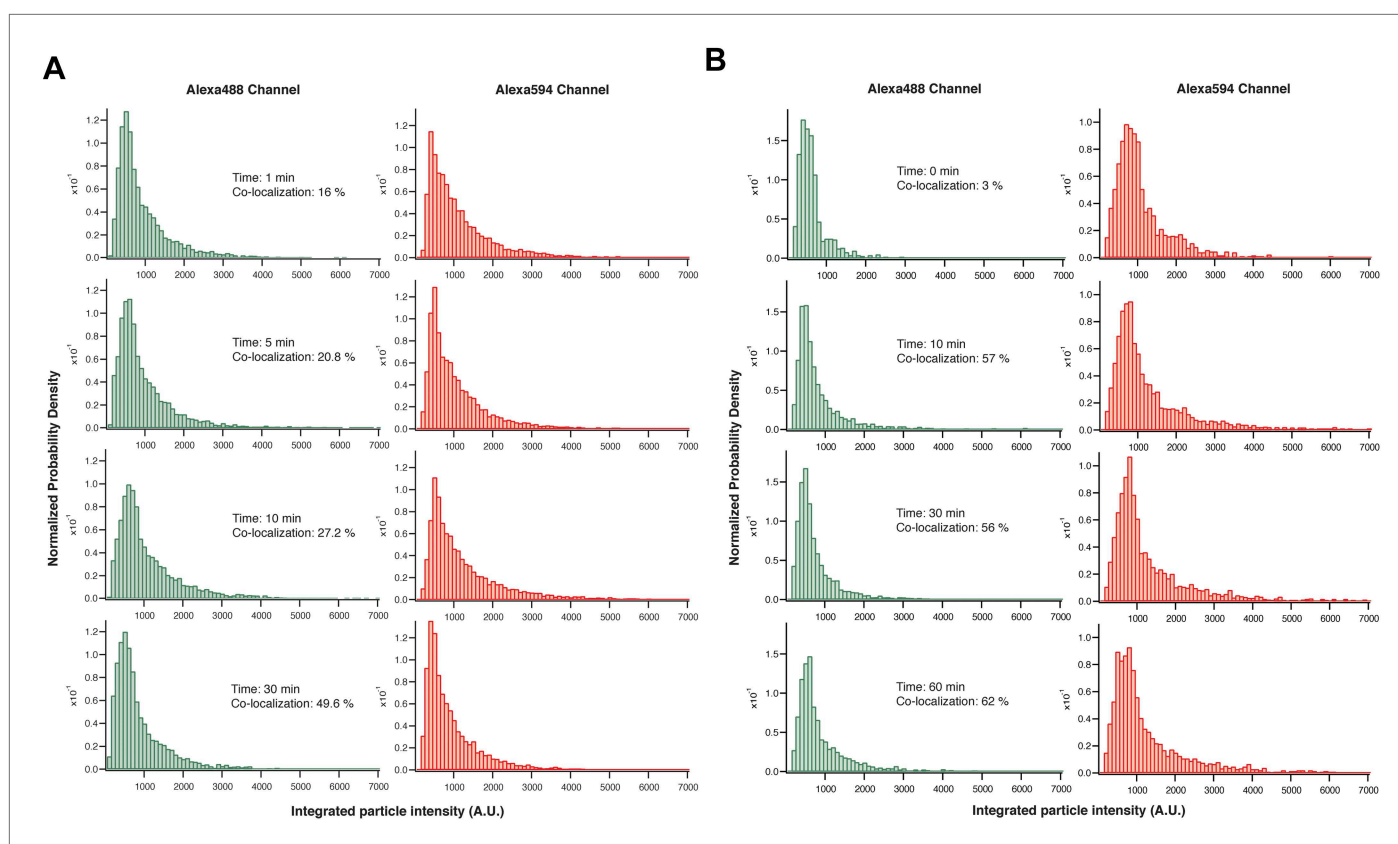


Figure 2—figure supplement 3. Intensity distribution analysis of single-molecule images.

DOI: [10.7554/eLife.01610.007](https://doi.org/10.7554/eLife.01610.007)

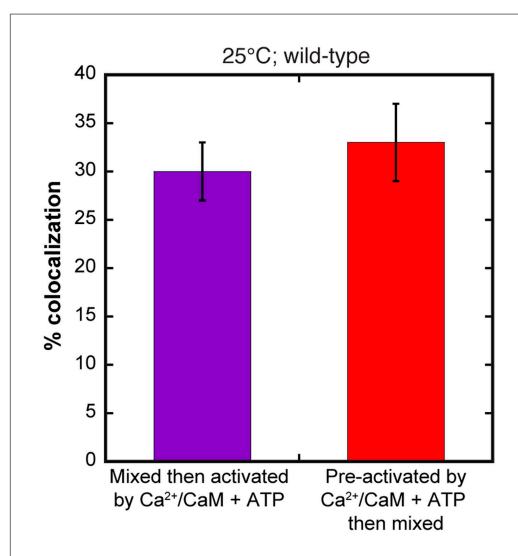


Figure 2—figure supplement 4. Comparison of activation methods and subunit exchange.

DOI: [10.7554/eLife.01610.008](https://doi.org/10.7554/eLife.01610.008)

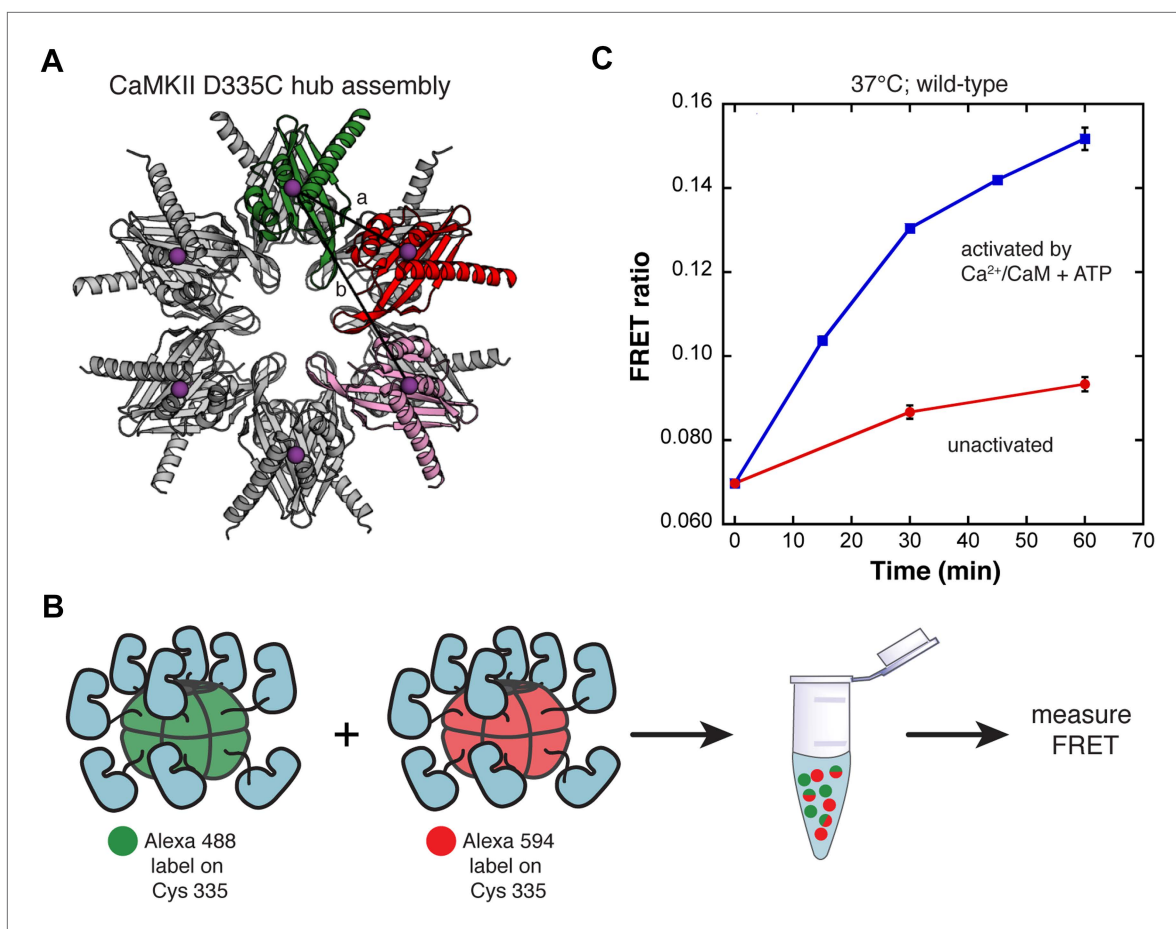


Figure 2—figure supplement 5. FRET mixing experiments corroborate single-molecule results.

DOI: [10.7554/eLife.01610.009](https://doi.org/10.7554/eLife.01610.009)

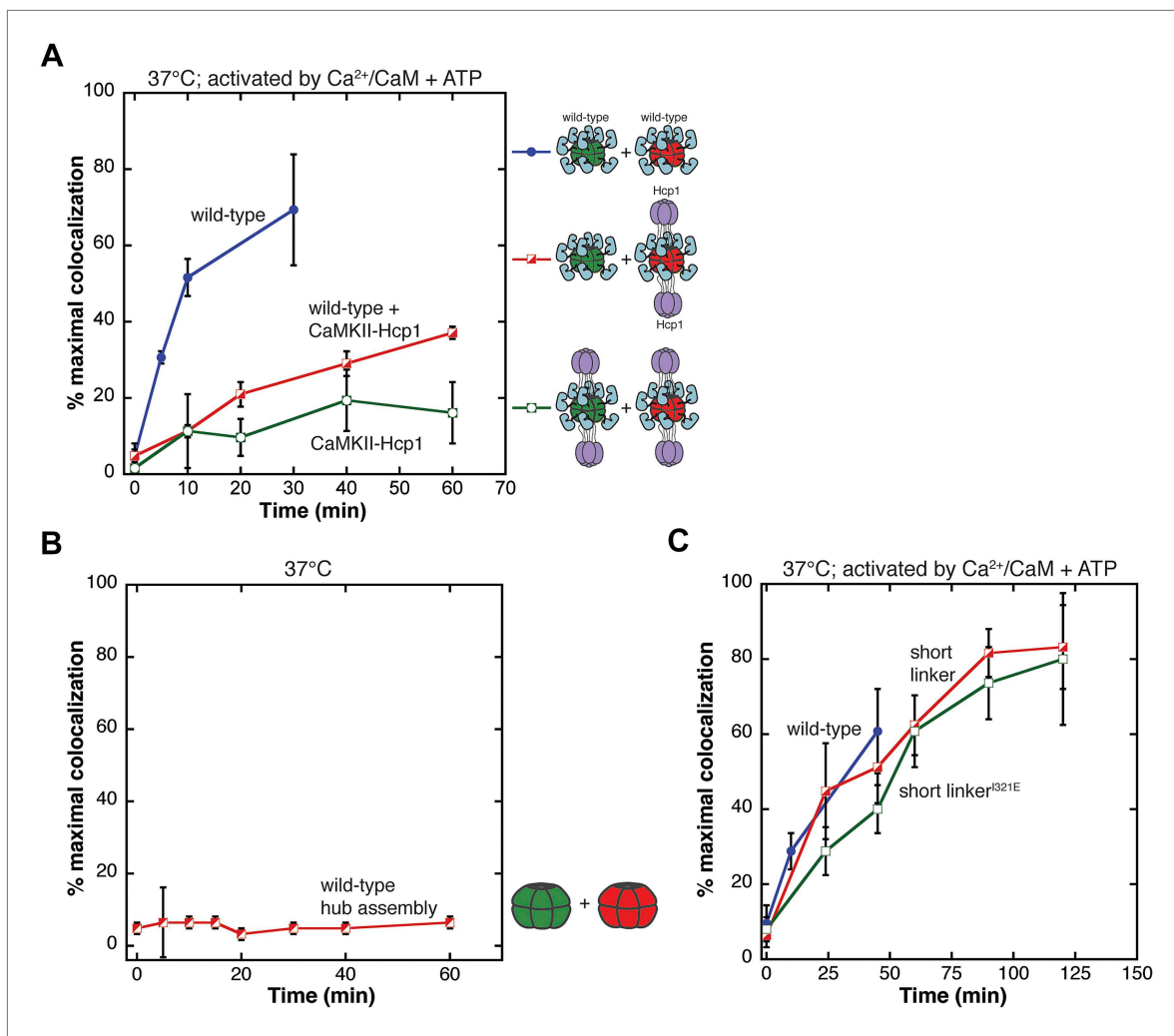


Figure 3. Analysis of the exchange process. **(A)** Single-molecule experiments show that fusion of CaMKII to a hexameric protein (Hcp1) slows the rate of colocalization. All samples are activated with $\text{Ca}^{2+}/\text{CaM}$ and ATP and mixing is done at 37°C. Mixing activated wild-type CaMKII yields about 70% of maximal colocalization (blue). Mixing wild-type and CaMKII-Hcp1 shows a marked decrease in colocalization (red). Mixing CaMKII-Hcp1 species results in nearly no colocalization (green). **(B)** The isolated hub assembly does not result in colocalization when labeled subunits are mixed. **(C)** Deletion of the variable linker region does not affect colocalization significantly. Comparison of the short-linker construct (red), short-linker construct mutated at the hub-kinase interface (green), and wild-type CaMKII (blue) shows minimal differences in colocalization.

DOI: [10.7554/eLife.01610.010](https://doi.org/10.7554/eLife.01610.010)

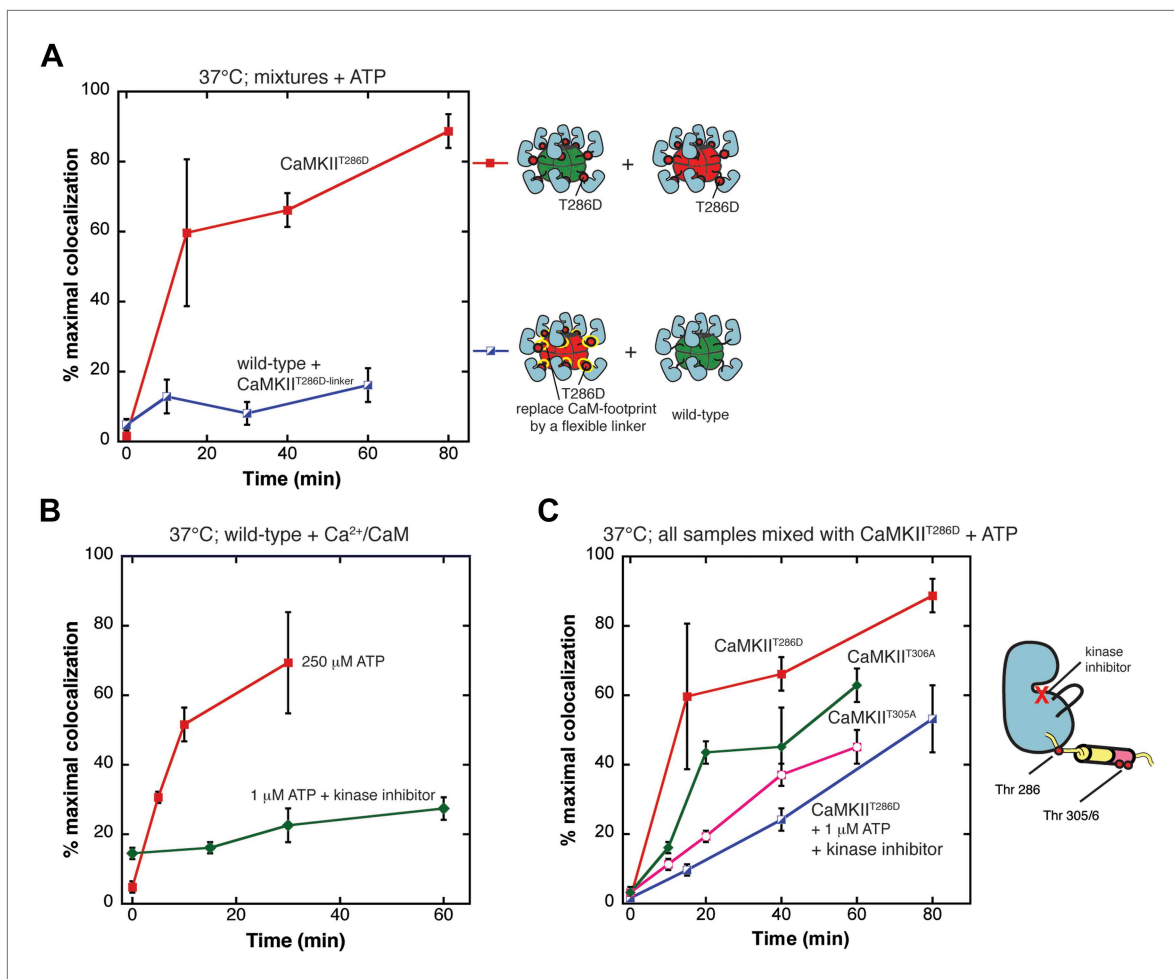


Figure 4. Phosphorylation of the calmodulin-recognition element is crucial for exchange. **(A)** Mixing CaMKII^{T286D} in the absence of Ca²⁺/CaM results in robust colocalization (red). Mutating the CaM-recognition element (R3) reduces colocalization significantly (blue). **(B)** Both mixing experiments shown use wild-type CaMKII in the presence of Ca²⁺/CaM. The addition of a kinase inhibitor and 1 μ M ATP significantly reduces colocalization (green) compared to a condition with full kinase activity (250 μ M ATP, no kinase inhibitor) (red). **(C)** All species are mixed with CaMKII^{T286D} in the absence of Ca²⁺/CaM. Compared to the colocalization resulting from mixing CaMKII^{T286D} (red), mixing CaMKII^{T286D} in the presence of a kinase inhibitor results in reduced colocalization (blue). Replacement of either Thr 305 or Thr 306 by alanine also results in a reduction in colocalization (pink and green, respectively).

DOI: [10.7554/eLife.01610.011](https://doi.org/10.7554/eLife.01610.011)

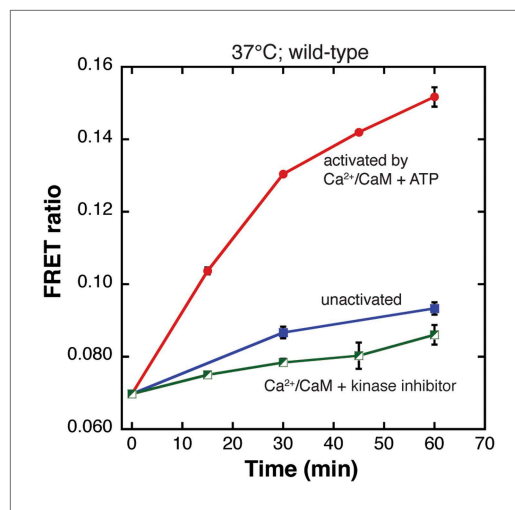


Figure 4—figure supplement 1. Kinase activity is crucial for exchange.

DOI: [10.7554/eLife.01610.012](https://doi.org/10.7554/eLife.01610.012)

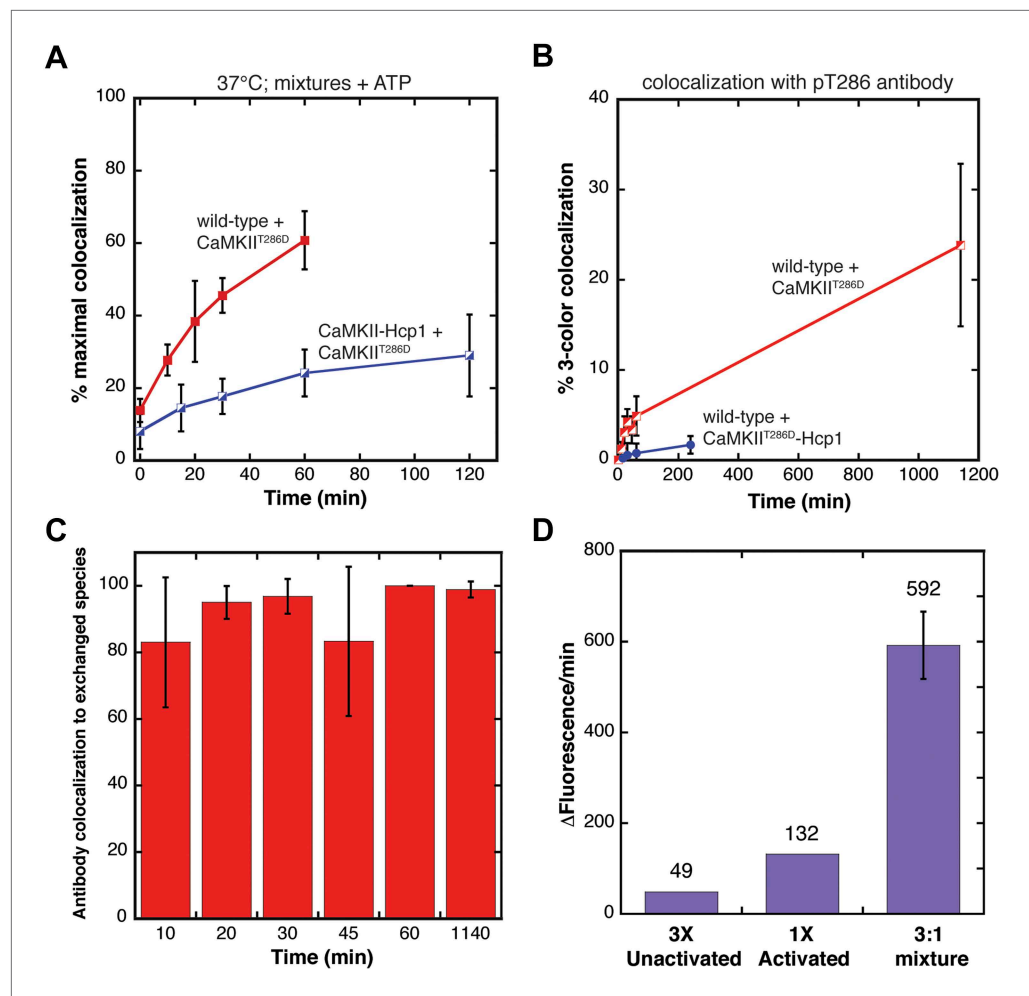


Figure 5. Evidence for the spread of phosphorylation into unactivated holoenzymes. **(A)** Both mixing experiments shown use wild-type CaMKII in the presence of $\text{Ca}^{2+}/\text{CaM}$ and ATP. CaMKII^{T286D} mixed with unactivated wild-type CaMKII results in high colocalization (red). This colocalization is suppressed by the addition of the Hcp1 module (CaMKII-Hcp1; blue). **(B)** Levels of pThr286 labeling in each mixing experiment from **(A)**. The pThr286 antibody is modified with Alexa 647, which is then added to the mixed samples. Subsequent analysis is for 3-color colocalization between Alexa dyes 488, 594, and 647. The phosphorylation spreads significantly more in the CaMKII^{T286D} sample (red) compared to the sample mixed with CaMKII^{T286D}-Hcp1 (blue). **(C)** There is colocalization of the pThr286 antibody with particles that have both Alexa 488 and 594, indicating that the antibody is only binding to those CaMKII holoenzymes that have already exchanged subunits. The graph shows the fraction of antibody label that is colocalized to particles that contain both the red and green fluorophores. Note that this fraction is close to 100%. **(D)** Kinase activity against a peptide substrate (syntide) was monitored in solution using the ADP Quest assay, where the fluorescence of resorufin is an indicator of ATP consumption. The reaction rates are plotted for three separate samples. First, 3 μl of an unactivated CaMKII sample, then 1 μl of an activated CaMKII sample (both are at the same final protein concentration), and finally a mixture of these components. The value of the reaction rate is indicated above each bar. It is clear that the reaction rate in the mixture is higher than just the addition of the rates of the individual components.

DOI: [10.7554/eLife.01610.013](https://doi.org/10.7554/eLife.01610.013)

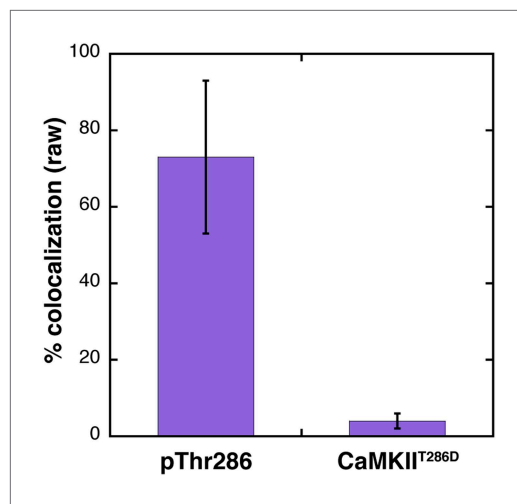


Figure 5—figure supplement 1. Controls for the pThr286 antibody.
DOI: [10.7554/eLife.01610.014](https://doi.org/10.7554/eLife.01610.014)

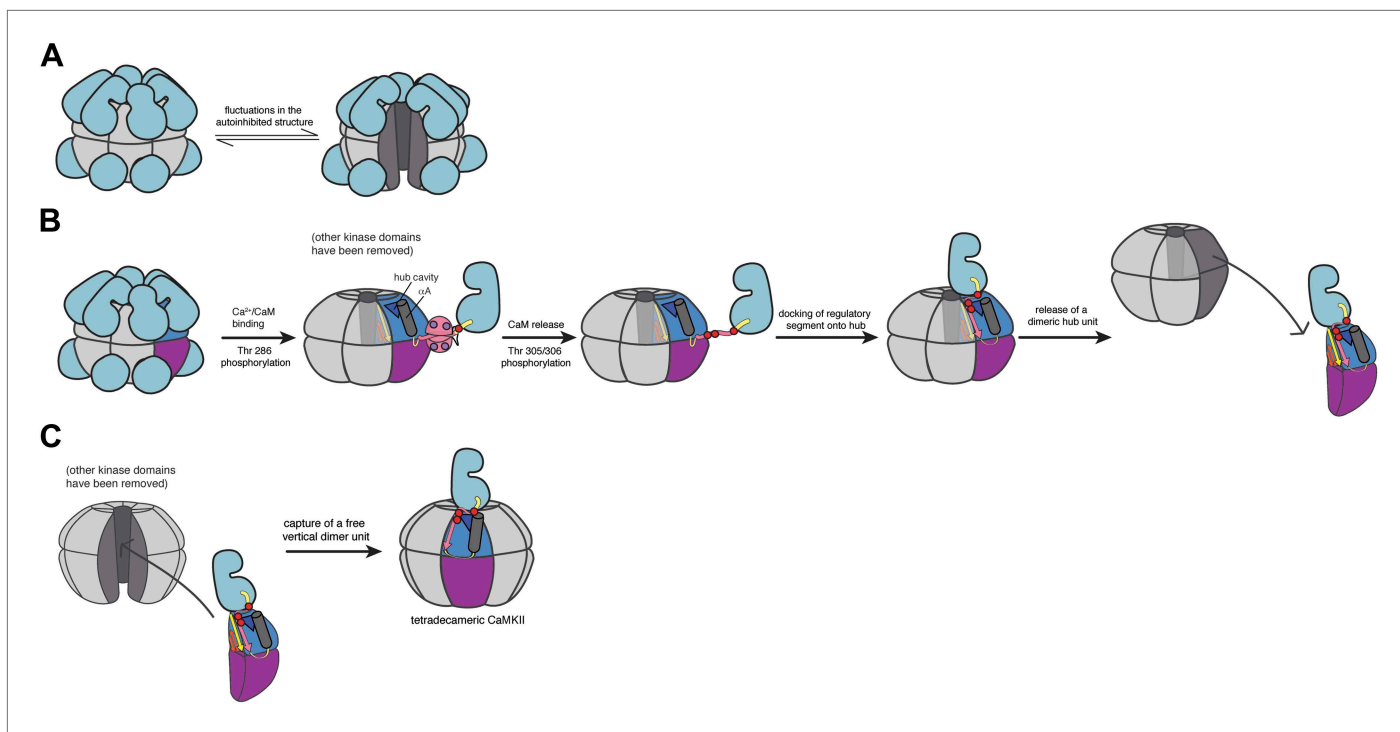


Figure 6. Schematic of a potential mechanism for subunit exchange in CaMKII. **(A)** In the unactivated state of CaMKII, the dodecameric hub domain undergoes fluctuations, which leads to transient lateral openings between vertical dimeric units. **(B)** Upon Ca²⁺/CaM binding, Thr 286 is trans-phosphorylated. For simplicity, just one kinase domain is depicted. When calcium levels drop, CaM falls off and Thr 305 and Thr 306 are subsequently phosphorylated. The now-released regulatory segment is free to bind the open β sheet of its own hub domain. This brings residues 305/306 in close proximity to the hub cavity (blue triangle), which houses the three conserved Arg residues. Binding of the regulatory segment induces a crack to open in the hub domain, which exposes the Arg residues to the phosphate groups. We reason that phosphorylation of the regulatory segment leads to an interaction between the R3 element and the hub domain that weakens the lateral association between hub domain dimers, leading to their release from one holoenzyme. **(C)** Fluctuations in the autoinhibited holoenzyme create a hub assembly that resembles a 'C' shaped structure. This fluctuation may allow the capture of a vertical dimer that has been released from an active holoenzyme. The drawing depicts the adoption of a tetradecameric structure upon docking of an incoming vertical dimer, which may be an intermediate in the exchange process. As discussed in the main text, we have no direct experimental evidence at present concerning the exchange process. We cannot, therefore, rule out alternative mechanisms, such as those involving a transient aggregation of holoenzymes prior to exchange.

DOI: [10.7554/eLife.01610.015](https://doi.org/10.7554/eLife.01610.015)

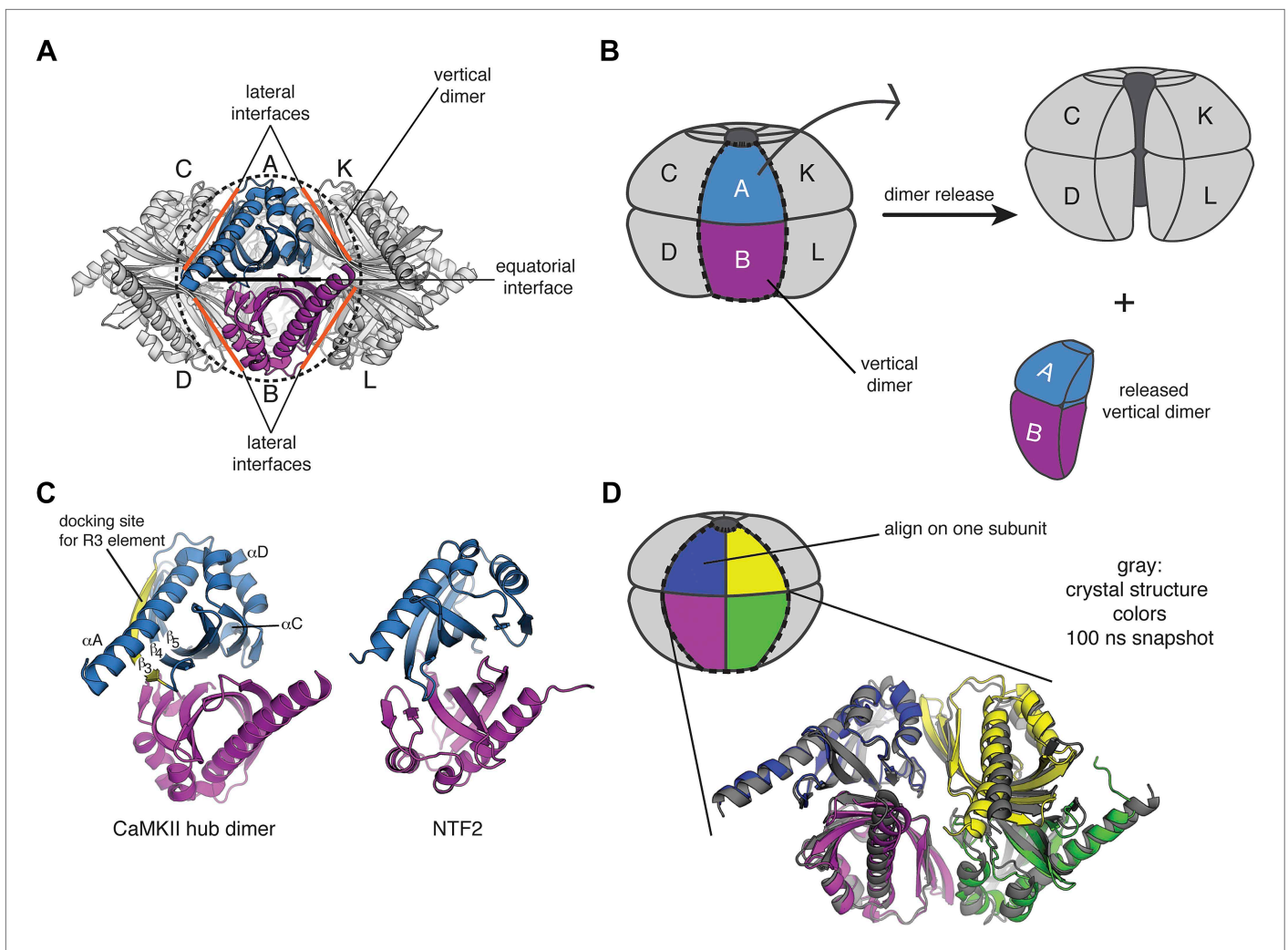


Figure 7. A vertical dimeric unit of the CaMKII assembly may be the unit of exchange. **(A)** The CaMKII hub assembly can be described as a set of six vertical dimers, and each dimer is labeled as A/B; C/D; etc. One of these dimers (A/B) is highlighted in blue/magenta (black dashed line). The lateral interfaces and equatorial interface for this dimer are indicated by orange and black lines, respectively. **(B)** A schematic diagram that indicates how one vertical dimer may be released from the holoenzyme. **(C)** The structure of the vertical hub dimer from CaMKII is shown in comparison to a dimer of NTF2 (PDB codes: 2UX0 and 1OUN, respectively). The notation for the secondary structural elements of the CaMKII hub domain are shown. **(D)** A molecular dynamics simulation was started from the dodecameric crystal structure of the hub domain (PDB code: 2UX0). The starting crystal structure is overlaid with an instantaneous structure from the molecular dynamics trajectory at 100 ns, aligning onto just one subunit (indicated on the schematic). It is clear that the vertical dimeric unit is relatively stable (blue/magenta), but there is a significant change in the relative positioning of the blue/magenta dimer with respect to the yellow/green dimer. This indicates that the lateral interfaces are more dynamic than the equatorial interfaces.

DOI: [10.7554/eLife.01610.016](https://doi.org/10.7554/eLife.01610.016)

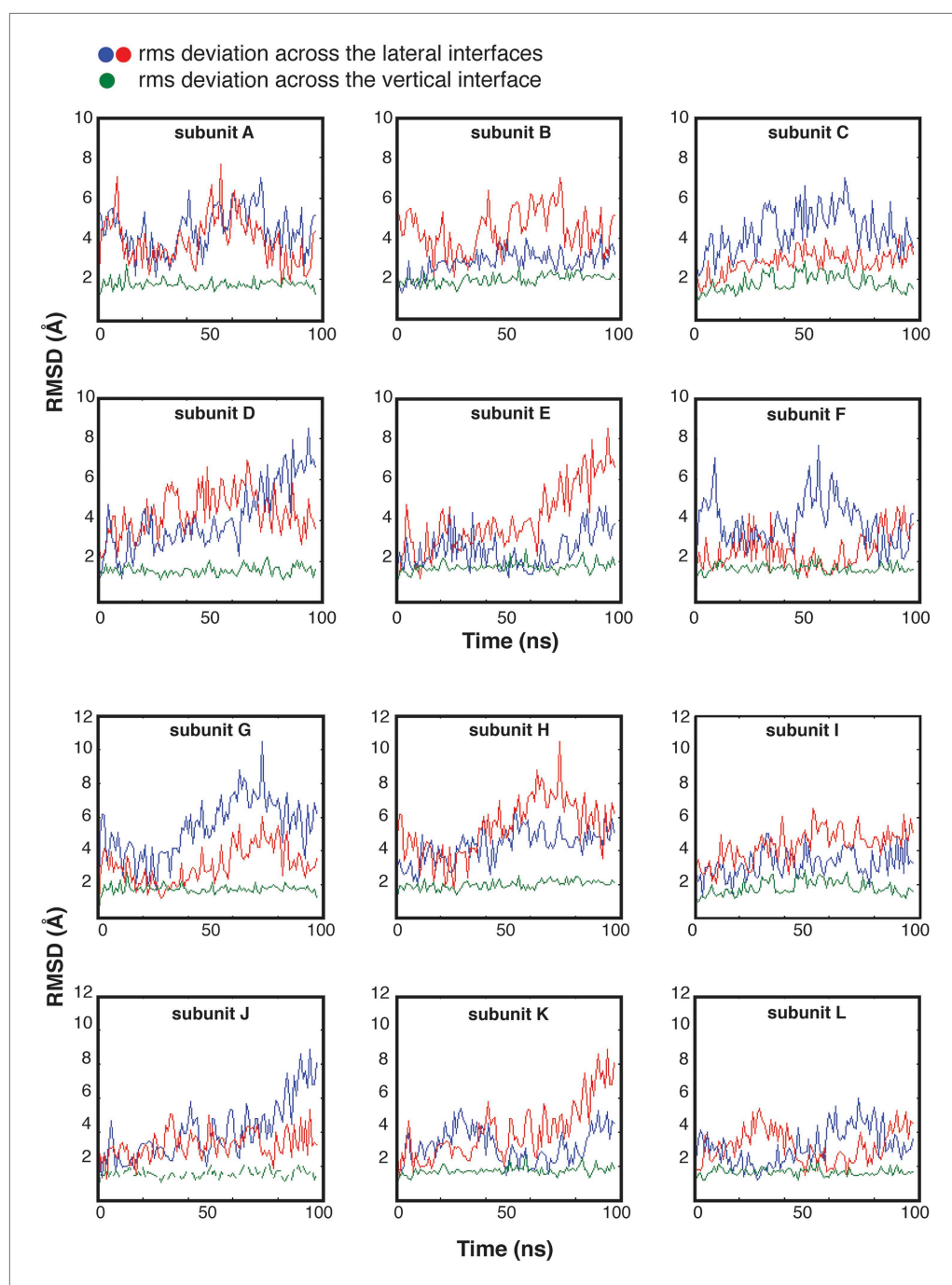


Figure 7—figure supplement 1. Molecular dynamics simulations suggest that the contacts across equatorial interfaces are stronger than those across the lateral interfaces.

DOI: [10.7554/eLife.01610.017](https://doi.org/10.7554/eLife.01610.017)

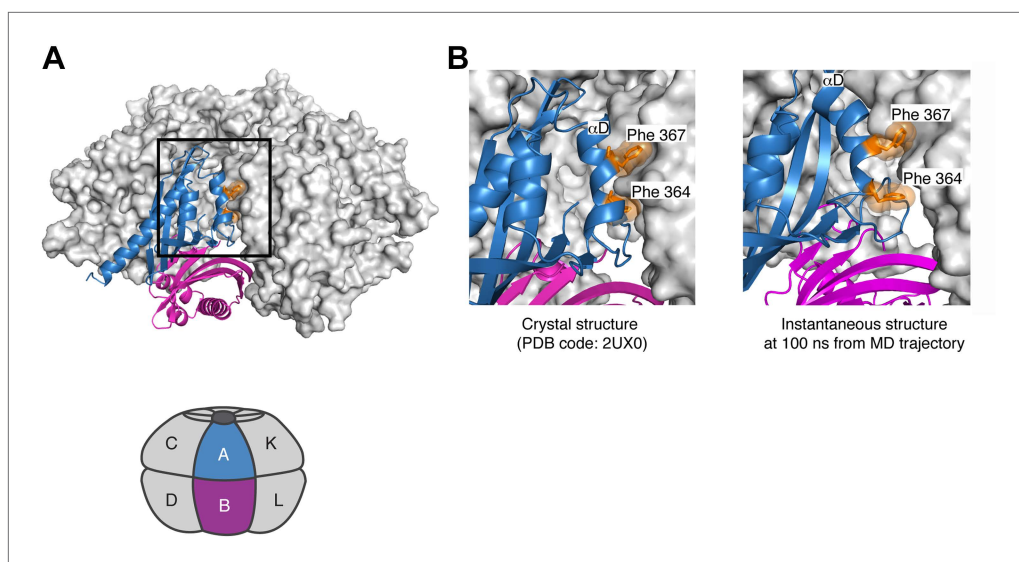


Figure 8. Strain associated with the closed ring formed by the dodecameric hub assembly of CaMKII. During the simulation of the CaMKII γ dodecamer, the sixfold symmetry of the hub assembly breaks down due to the tightening of some of the lateral interfaces and loosening at others. **(A)** A view of one of the lateral interfaces, with a close-up view in **(B)**. At this interface, the residues on helix α D in one subunit and the β 4 and β 5 strands on the other are splayed apart after 100 ns of simulation, so that the sidechains of Phe 364 and Phe 367, which are buried in the crystal structure (left) and more stable interfaces, are now partially solvent exposed (right). These results suggest that the constraint of ring closure prevents the simultaneous optimization of all of the lateral interfaces.

DOI: [10.7554/eLife.01610.018](https://doi.org/10.7554/eLife.01610.018)

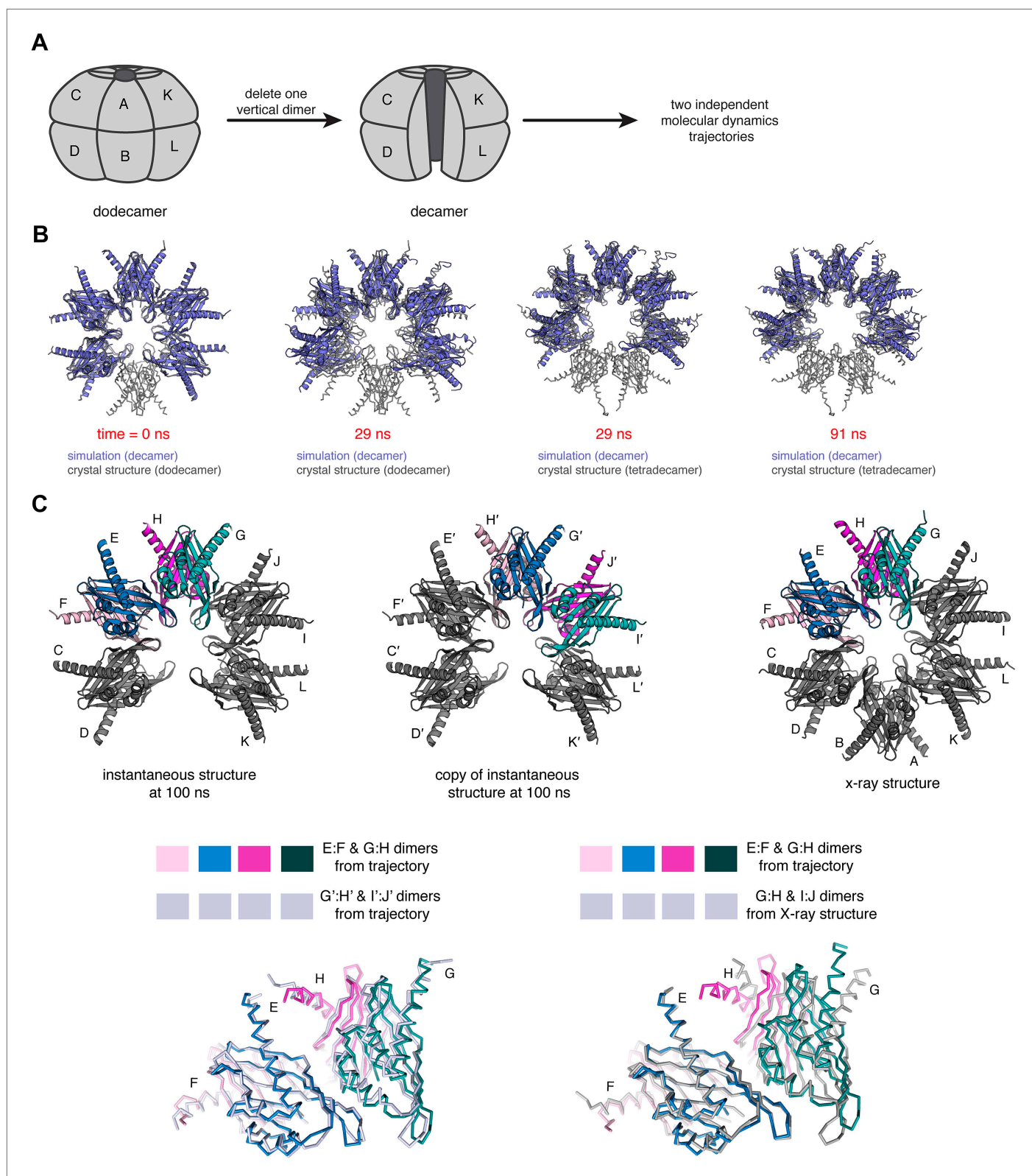


Figure 9. Molecular dynamics simulations of an open-ringed (decameric) hub assembly. **(A)** The dodecamer consists of six vertical dimers, denoted A:B, C:D...K:L. The decamer used in the simulations is created by removing the A:B dimer. **(B)** We initiated two independent molecular dynamics trajectories from this decameric structure and the results for one are shown in this diagram. Instantaneous structures from this simulation are shown overlaid with the crystal structure for either the dodecameric (PDB code: 2UX0) or tetradecameric (PDB code: 1HKX) hub assembly. At 29 ns, it is clear that the decamer

Figure 9. Continued on next page

Figure 9. Continued

has relaxed to the tetradecameric conformation, with further opening evident at 91 ns. **(C)** There are two internal vertical interfaces in the decamer, between the E:F and G:H vertical dimers and between the G:H and I:J vertical dimers (colored in the structural diagram shown at the top). To demonstrate the convergence of the two vertical interfaces to an arrangement that is distinct from the interfaces in the crystal structure, we calculated the displacement of atomic positions in interfacial subunits after the E:F/G:H and G:H/I:J interfaces were brought into spatial alignment using only one subunit, for a series of instantaneous structures extracted from the trajectories. To do this, we made a copy of the trajectory. The subunits in the original are labeled C through K, and in the copy they are labeled C' through K'. The two internal interfaces (E:F/G:H and G:H/I:J) are brought into alignment by superimposing subunit E from the original onto subunit G' of the copy of the trajectory, for pairs of structures at the same point in the trajectory. The overlaid structures are shown at the bottom left. The close overlap shows that the two vertical interfaces in this instantaneous structure are similar. We then aligned subunit E of the instantaneous structure with subunit G of the crystal structure (bottom right). The poor overlap between the crystal structure and the instantaneous structure is evident.

DOI: [10.7554/eLife.01610.019](https://doi.org/10.7554/eLife.01610.019)

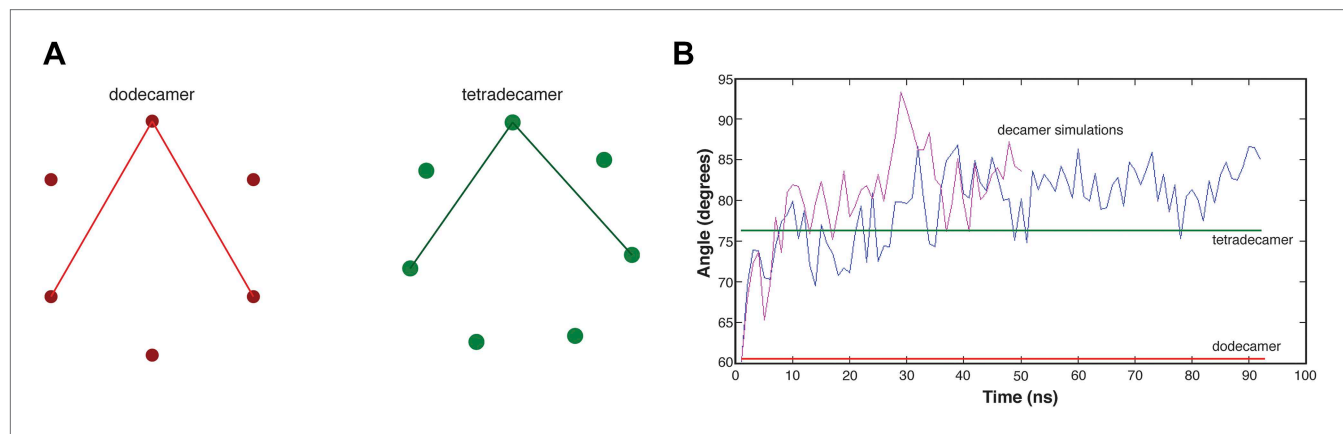


Figure 9—figure supplement 1. Relieving strain in the dodecameric ring tends towards a tetradecameric conformation.

DOI: [10.7554/eLife.01610.020](https://doi.org/10.7554/eLife.01610.020)

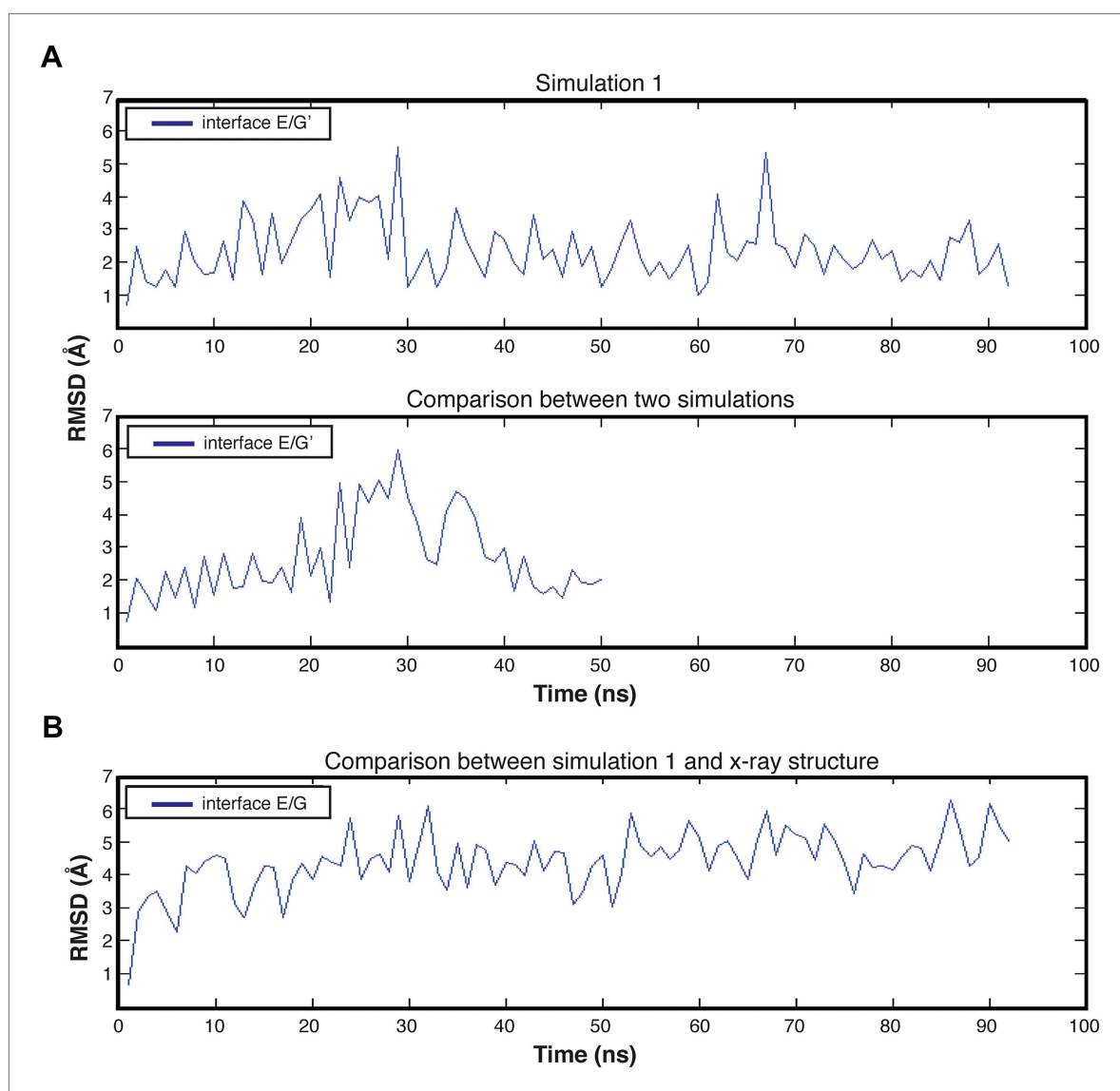


Figure 9—figure supplement 2. Structural changes during molecular dynamics, showing the relaxation of the decamer to a specific interfacial arrangement.

DOI: [10.7554/eLife.01610.021](https://doi.org/10.7554/eLife.01610.021)

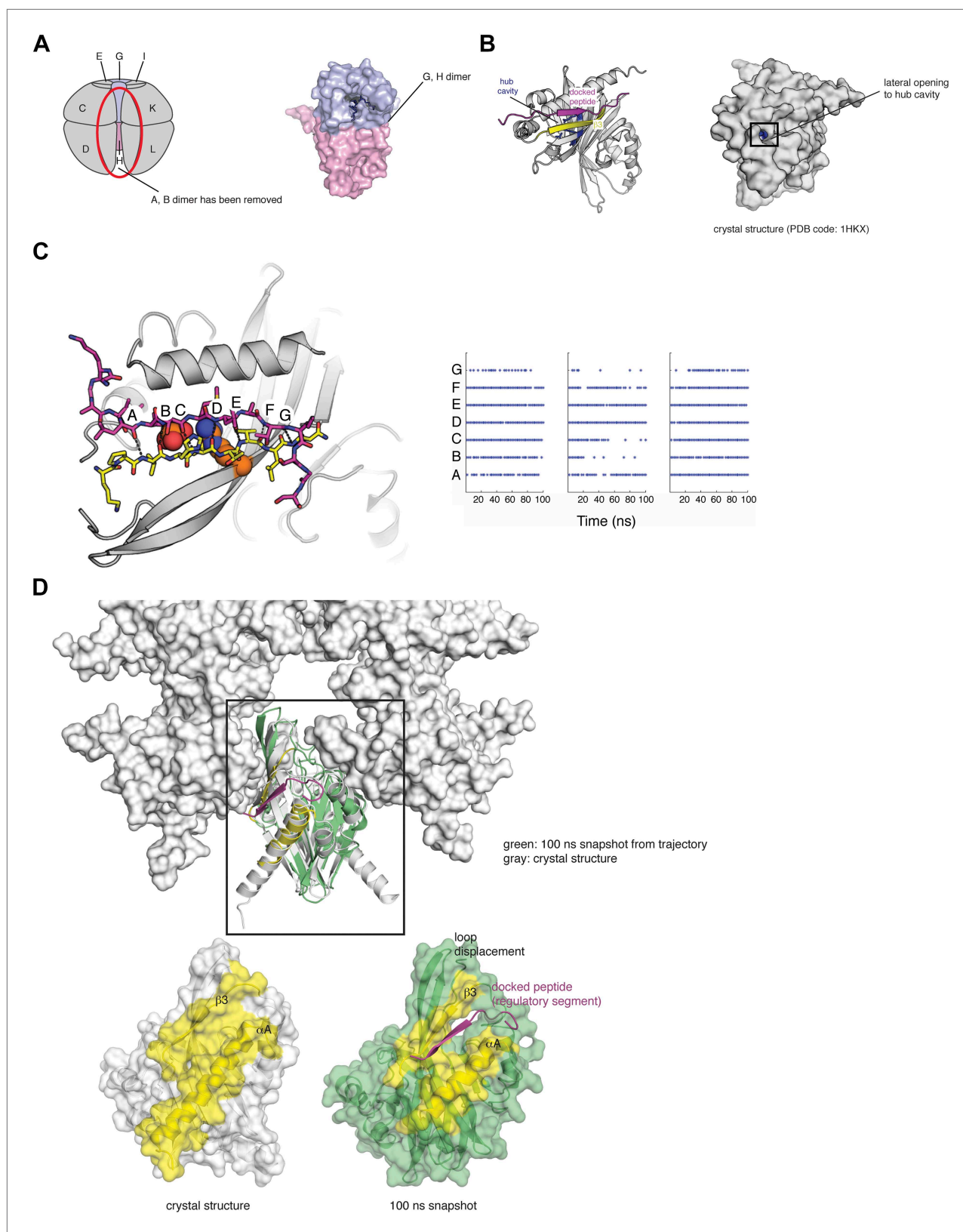


Figure 10. Side entrance to the hub cavity and docking of the regulatory segment onto the hub. **(A)** One vertical dimer unit has been removed from the side view of the decameric hub assembly (shown as a schematic on the left). There is limited access to this cavity in the context of the holoenzyme. A close up of the G/H dimer from the crystal structure of CaMKII γ (PDB code: 2UX0) is highlighted in blue/pink (right). There are three arginine residues Figure 10. Continued on next page

Figure 10. Continued

that are located deep within the hub cavity (residues 403, 423, and 439), and these are highly conserved in CaMKII. **(B)** Shown is a vertical dimer from the mouse CaMKII α crystal structure (PDB code: 1HKX). The crystal structure is shown in cartoon representation (left) with the regulatory segment (magenta) docked onto β 3 (yellow). On the right, the crystal structure is shown as a surface representation where the hub cavity that contains the arginine residues (blue) is apparent through a small crack (between α A and β 3), which we refer to as the lateral opening. **(C)** The regulatory segment (magenta) was docked onto β 3 in the hub assembly (yellow). This docked model was used to generate three independent molecular dynamics trajectories (100 ns each). In each of these trajectories the R3 element retains the hydrogen bonding pattern (right) that is consistent with its incorporation into the β sheet of the hub domain and the phosphate group maintains its proximity to the sidechain of Arg 403, suggesting that this interaction is plausible. Each trajectory was sampled every 2 ns and each dot represents the formation of a hydrogen bond (<3.5 Å). **(D)** Peptide binding disrupts lateral contacts within the hub domain. Docking of the regulatory segment peptide (magenta) prevents the crack between α A (yellow) and β 3 (yellow) from closing. This is coupled to changes in the loops that make lateral contacts with the adjacent vertical dimers. This disruption may be sufficient to allow the release of a vertical dimer unit from the hub assembly and facilitate the exchange of subunits between holoenzymes.

DOI: [10.7554/eLife.01610.022](https://doi.org/10.7554/eLife.01610.022)